Spectrum- and time-resolved investigation of pre-excited argon atoms

Fangbo Zhang,[1,2] Zhaoxiang Liu,[1,2] Jinping Yao,[1,*] Bo Xu,[1,2] Jinming Chen,[1,2,4] Yuexin Wan,[1,2] Wei Chu,[1] Zhenhua Wang,[3] Ya Cheng,[1,3,5] and Zhizhan Xu[1,†]

[1]*State Key Laboratory of High Field Laser Physics, Shanghai Institute of Optics and Fine Mechanics, Chinese Academy of Sciences, Shanghai 201800, China*

[2]*Center of Materials Science and Optoelectronics Engineering, University of Chinese Academy of Sciences, Beijing 100049, China*

[3]*State Key Laboratory of Precision Spectroscopy, East China Normal University, Shanghai 200062, China*

[4]*School of Physical Science and Technology, ShanghaiTech University, Shanghai 200031, China*

[5]*Collaborative Innovation Center of Extreme Optics, Shanxi University, Taiyuan, Shanxi 030006, China*

(Received 2 October 2019; published 23 December 2019)

It has been observed that in a pre-excited medium produced by femtosecond laser pulses, nonlinear interaction can be dramatically enhanced. The underlying mechanism is still under debate because of the lack of detailed information on the species, energy states, and temporal dynamics of the excited medium. Here, we report a dramatic enhancement of seventh-harmonic generation in pre-excited argon atoms. By measuring the evolution of the enhanced signal with the propagation distance, we are able to separate the contributions from the improved phase matching and the enhanced nonlinear susceptibility. The time- and spectrum-resolved measurements clearly show that generation of excited states is responsible for the enhanced nonlinear susceptibility. The maximum population of excited states on the picosecond and nanosecond timescales can be attributed to two possible pathways.

DOI: 10.1103/PhysRevA.100.063425

I. INTRODUCTION

Nonlinear frequency conversion during femtosecond laser filamentation in gaseous media has been intensively investigated due to its important implications for generation of coherent light sources and remote sensing [1–6]. So far, the typical efficiency of third-harmonic generation (THG) in air is measured to be ∼0.2% [2]. Further enhancement of optical nonlinearity in gaseous media is a long-pursued goal of researchers, which is usually realized by either optimizing the pump laser field [7,8] or manipulating the propagation medium and phase matching [9–29]. Pre-excitation of gases with intense laser pulses, as an efficient all-optical method for tailoring the nonlinear medium, has attracted considerable interest in the recent decade [14–20,23–25,27–29]. When a femtosecond laser pulse passes through a gaseous plasma generated by another femtosecond pulse, one has observed more than two orders of magnitude enhancement of THG in various atomic and molecular gases [14–17,20]. It has been experimentally demonstrated that the technique enables generation of intense vacuum ultraviolet pulses at 89 nm via low-order nonlinear processes excited by ultraviolet femtosecond laser pulses [24]. Moreover, the method has been applied to enhance the yield of high-order harmonics [28,29].

The mechanism of such a dramatic enhancement has motivated many interesting studies [17,19,25,27,30–34]. Basically, the proposed scenarios can be divided into two categories. One is attributed to the enhanced nonlinear susceptibility in the bulk plasma [30,31] or in the excited atoms and molecules [25,27,33,34]. The other is attributed to the improved phase matching [17,19,32]. Specifically speaking, the pre-excited medium suppresses the Gouy-phase-induced destructive interference of the harmonic radiation before and after the focus. Up to now, there is still lack of a unified understanding for the enhancement effect. Furthermore, the gaseous excitation will produce abundant species, e.g., plasma, excited atoms, molecules, and ions, etc. All of them could give rise to the enhanced nonlinear polarization. Therefore, a convincing explanation requires knowing the information on the species, energy states, and dynamics of the excited medium, which, however, is missing in previous studies.

In this work, we experimentally studied the enhancement of seventh (7th)-harmonic generation in the pre-excited medium. By measuring the evolution of the enhanced signal with the propagation distance, we distinguished the contributions from the improved phase matching and the enhanced nonlinear susceptibility. The improved phase matching is manifested as further increase of the harmonic signal after the focus, whereas the higher nonlinear susceptibility in the excited medium makes the harmonic signal at each propagation position stronger than that without the prepulse. Particularly, with the transient absorption spectroscopy, we performed spectrum- and time-resolved measurements for the pre-excited medium. It was demonstrated that the $3p^5 4s$ excited state of argon plays a key role in the enhanced optical nonlinearity. The possible pathways to generating the excited state were discussed.

*jinpingmrg@163.com
†zzxu@mail.shcnc.ac.cn

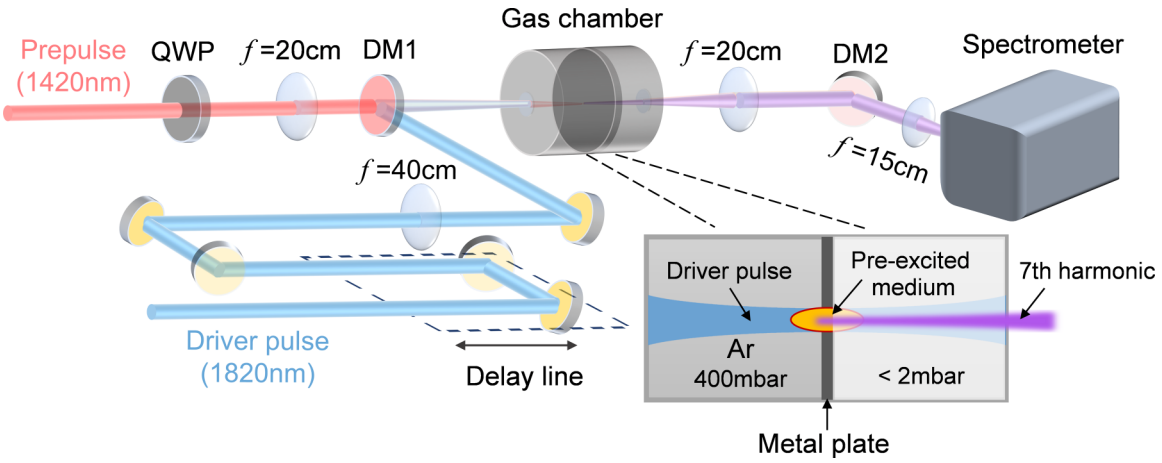

FIG. 1. Schematic diagram of the experimental setup. The inset indicates the side view of the gas chamber with a pressure gradient. QWP: quarter-wave plate; DM1: dichroic mirror with high reflectivity around 1820 nm and high transmission around 1420 nm; DM2: dichroic mirror with high reflectivity around 260 nm and high transmission around 1420- and 1820-nm wavelengths.

II. EXPERIMENTAL SETUP

The experiment setup is shown in Fig. 1. An optical parameter amplifier (OPA), which was pumped by an 800-nm, 6-mJ, 40-fs, 1-kHz Ti:sapphire laser system (Legend Elite-Duo, Coherent, Inc.), can provide midinfrared femtosecond laser pulses. The signal beam of the OPA with a center wavelength of 1420 nm was used as the prepulse to excite the gaseous medium. The corresponding idler beam centered at 1820 nm served as the driver pulse to induce 7th-harmonic generation. The energy of the prepulse and the driver pulse was ∼1 and 0.3 mJ, respectively. The prepulse was changed to circular polarization using a quarter-wave plate to suppress its supercontinuum background and odd-order harmonics. The two beams were collinearly combined using a dichroic mirror (DM1), and were focused into a gas chamber filled with 400 mbar argon gas by an $f = 20$ cm lens and an $f = 40$ cm lens, respectively. Both lenses were mounted on the translation stages to optimize their focal positions. The prepulse induced a 6-mm-long plasma channel near the focus. The time delay of the two beams was controlled by a 1.6-m-long linear stage, which allows for changing the relative delay from a femtosecond to a nanosecond timescale. The zero delay was determined by observing the strongest mixing frequency signal of two laser pulses in the argon gas. The 7th-harmonic signal of the driver laser was completely collected into an imaging spectrometer (Shamrock 500i, Andor) using a lens. To improve the signal to noise ratio, the harmonic signal near 260 nm and the residual midinfrared lasers were separated using another dichroic mirror (DM2). The relative intensity of the 7th harmonic was obtained by integrating the measured spectrum.

III. EXPERIMENTAL RESULTS AND DISCUSSION

A. Dramatic enhancement of 7th-harmonic generation

The free propagation of the 1820-nm driver pulses in the gas chamber usually generates odd-order harmonic radiations. First, we compared the 7th-harmonic spectra for cases with and without the prepulse. As indicated by a blue solid line in Fig. 2(a), the driver laser hardly generates the observable 7th harmonic. However, the harmonic radiation was dramatically enhanced when the prepulse was ahead of the driver pulse (i.e., positive delay). Figure 2(b) shows the enhanced harmonic signal as a function of the time delay of the two pulses. We can clearly see that the enhancement process can be divided into two stages. In the first stage, the 7th-harmonic signal shows rapid growth after zero delay and reaches its maximum at the time delay of ∼2 ps, and then decays with the further increase of the delay. The enhancement on the picosecond timescale has been observed in previous studies [14–20,23–25,28,29]. Interestingly, the harmonic signal increases again after 2 ns and reaches its second peak at the time delay of about 7 ns. The enhancement in the second stage is even more efficient than that in the first stage. A similar phenomenon was also observed in the third harmonic [25,27]. For comparison, the typical spectra of the 7th harmonic at the time delay of 2 ps and 7 ns are shown in Fig. 2(a), which are much stronger than that generated solely with the driver laser. The comparative measurements clearly reveal the crucial role of the prepulse on the harmonic enhancement.

B. Evolution of the enhanced 7th-harmonic with the propagation distance

To gain insight into the mechanism underlying the dramatic enhancement, we studied the evolution of the harmonic signal with the propagation distance. To perform this measurement, we designed a semi-infinite gas chamber by placing a 0.5-mm-thick metal plate near the focus. This method has been used in studies of high-harmonic generation and femtosecond filamentation [11,35–37]. The laser-drilled pinhole in the plate enables us to establish a pressure gradient from 400 mbar to <2 mbar, as shown in the inset of Fig. 1. With this method, we can truncate all nonlinear processes abruptly at defined positions, and ensure the harmonic signal passes through the pinhole. By changing the position of the metal plate with respect to the focal lens, we can measure the 7th-harmonic yield as a function of the propagation distance.

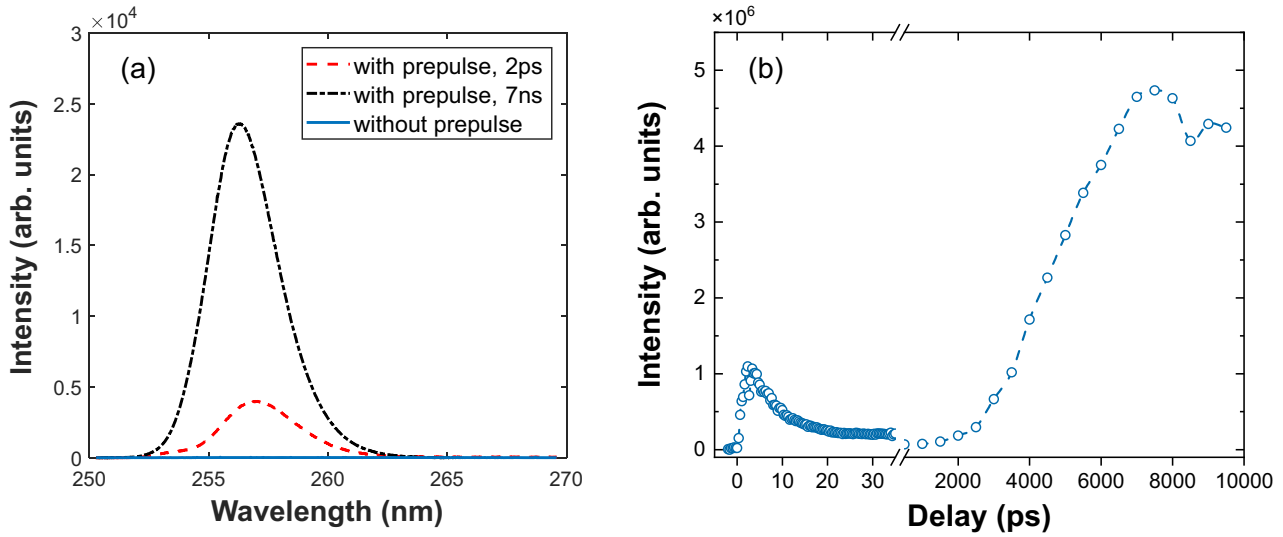

FIG. 2. (a) The comparison of 7th-harmonic spectra captured at the time delay of 2 ps (red dashed line) and 7 ns (black dash-dot line) with the harmonic spectrum obtained in the absence of the prepulse (blue solid line). (b) The intensity of the 7th harmonic as a function of the time delay between the prepulse and the driver pulse.

The measurement results are shown in Fig. 3(a). The relative positions of the pre-excited medium, the driver laser beam, and the metal plate are indicated in the inset. In this measurement, the focus of the driver laser is fixed at the center of the pre-excited medium. It can be seen that in the absence of the prepulse, the harmonic radiation excited by the driver pulse alone reaches its maximum near its focus. The reduction of the harmonic signal after the focus indicates the important influence of Gouy phase shift on 7th-harmonic generation. More specifically, the Gouy phase shift results in the destructive interference of the harmonic radiation before and after focus [38], so that extremely weak harmonic radiation is

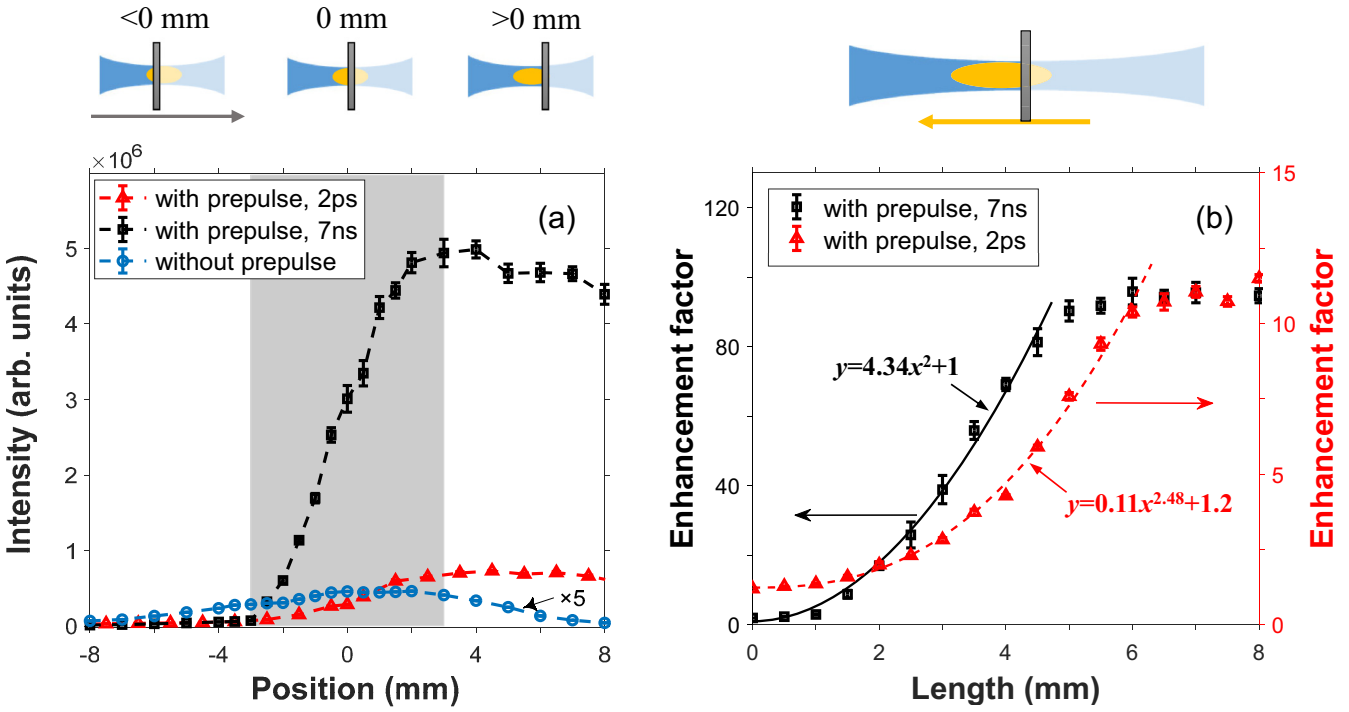

FIG. 3. (a) The evolution of the 7th-harmonic signal with the propagation distance. For clarity, the harmonic signals solely produced by the driver pulse are multiplied by a factor of 5. The shadow indicates the effective region of the pre-excited medium, and the position at 0 mm represents the focus of the driver laser. Inset: relative positions of the pre-excited medium, the driver laser, and the metal plate. In the measurement, the focus of the driver laser is fixed at the center of the pre-excited medium. (b) The enhancement factor of the 7th harmonic as a function of the length of the excited medium. The solid and dashed lines are numerical fits of experimental data. Inset: relative positions of the pre-excited medium, the driver laser, and the metal plate. In the measurement, the metal plate is fixed at the focus of the driver pulse.

observed at the exit. The injection of the prepulse fundamentally changes the evolution of the harmonic signal along the propagation direction. As demonstrated by red triangles and black squares in Fig. 3(a), both the harmonic signals captured at the delay of 2 ps and 7 ns show a rapid growth with the increased propagation distance, and almost remain constant beyond the pre-excited region. Apparently, the harmonic signal no longer decreases after the focus, indicating that the excited medium effectively suppresses the destructive interference caused by the Gouy phase shift. Since the modification of the Gouy phase shift takes place in both picosecond and nanosecond timescales, it cannot be completely attributed to the plasma effect [17,19]. It could be because the change of refractive index in the excited medium affects the propagation of the fundamental wave. In addition, it is noteworthy that the harmonic signal at each position of the excited medium is much stronger than that produced by the driver laser alone, implying that the excited gas has a higher nonlinear susceptibility. The comparative measurements in Fig. 3(a) clearly demonstrate that the enhancement of the 7th harmonic should be attributed to the joint contributions of the modified Gouy phase shift and the improved nonlinear susceptibility. Their contributions can be distinguished by examining the evolution of the 7th harmonic with the propagation distance.

We further study the independent contribution of the enhanced nonlinear susceptibility to the harmonic enhancement. To this end, the metal plate is fixed at the focus of the driver pulse, while the length of the excited medium is changed by moving the focal lens of the prepulse, as shown in the inset of Fig. 3(b). This experimental configuration enables us to minimize the influence of the Gouy phase shift. Meanwhile, the harmonic radiation produced by the driver pulses alone remains at its maximum. The enhancement factor is obtained by calculating the intensity ratio of the 7th harmonic generated with and without the prepulse. As shown in Fig. 3(b), the harmonic signals at the delay of 2 ps and 7 ns are increased by one and two orders of magnitude, respectively, which mainly originate from the enhanced nonlinear susceptibility as discussed later. Furthermore, the enhanced harmonic signal shows a nearly squared growth with the increase of the length, indicating that phase mismatch is negligible for seventh-harmonic generation in the excited medium [38]. Figure 3(b) also clearly shows that the harmonic signal will remain unchanged beyond the excitation region. It means that the harmonic radiation is mainly from the pre-excited medium.

C. Time- and spectrum-resolved measurements of the pre-excited medium

The experimental results in Fig. 3(b) clearly indicate the dramatic enhancement of the nonlinear susceptibility in the presence of the prepulse. Such an enhancement usually originates from the electronic resonance or generation of new species with a higher nonlinear susceptibility. However, the enhancement effect is independent of the driver wavelength [14–20,23–25,27–29], and can be observed in other noble gases. Thus, we can exclude the contribution of resonant effects. It is known that the excitation of argon atoms will generate the plasma, excited atoms, and ions, etc. To identify which one causes the harmonic enhancement, we performed both time- and spectrum-resolved measurements for the pre-excited medium with transient absorption spectroscopy. The 800-nm, 5-nJ, 40-fs laser pulses from the Ti:sapphire laser system, which serve as the probe beam, are injected into the pre-excited medium. It should be emphasized that the probe pulse is extremely weak to accurately measure the population dynamics. At proper time delays, we observed very sharp absorption dips in the probe spectrum. A typical absorption spectrum is shown in Fig. 4(a). We selected three dips, denoted as (1)–(3), which correspond to the transitions between two lower excited states of Ar atoms, i.e., $3p^5 4s \rightarrow 3p^5 4p$ [39], as illustrated in Fig. 4(b). The other dips

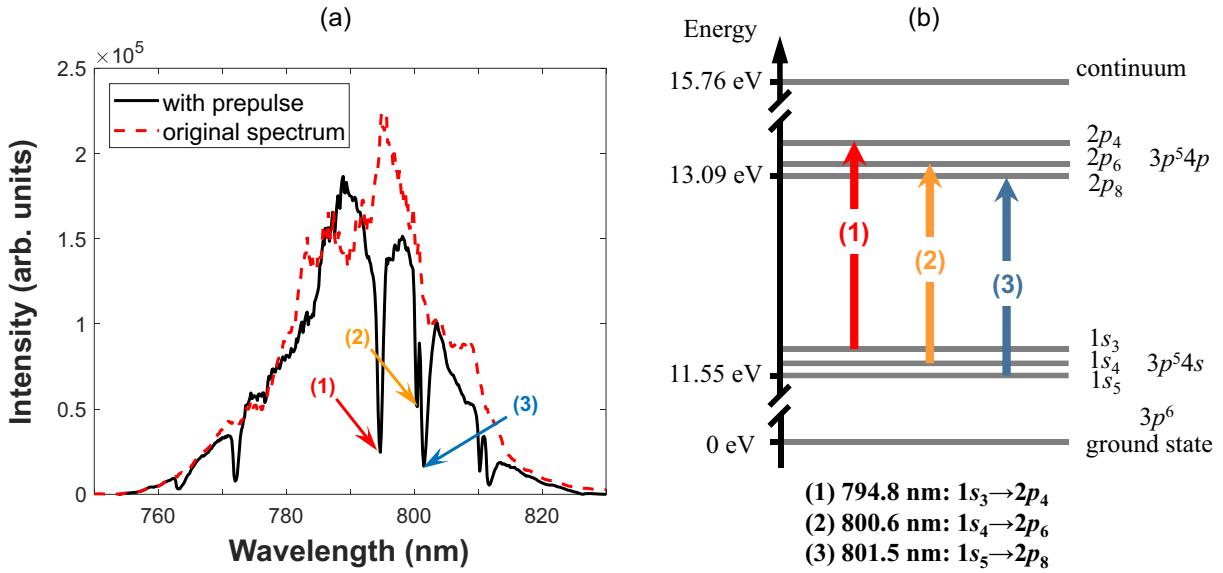

FIG. 4. (a) The absorption spectrum obtained by injecting a weak probe pulse into the pre-excited medium at the time delay of 7 ns. For comparison, the original probe spectrum is indicated by a red dashed line. (b) Energy-level diagram of three transitions corresponding to these absorption dips. The wavelengths corresponding to these transitions are indicated on the bottom.

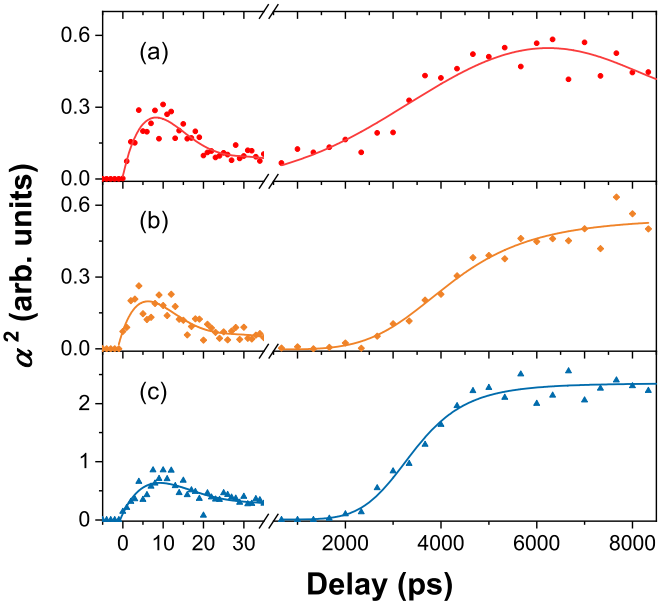

FIG. 5. The squared absorption coefficient (α^2) obtained at the wavelengths of (a) 794.8 nm (red dots), (b) 800.6 nm (orange diamonds), and (c) 801.5 nm (blue triangles) as a function of the time delay between the 1420-nm prepulse and the 800-nm probe pulse. The solid lines are the numerical fit of experimental data to guide the eyes.

in the absorption spectrum also originate from the transitions from sublevels of $3p^5 4s$ to sublevels of $3p^5 4p$, which will not be discussed here. These strong absorptions imply that atoms in the ground state are efficiently excited, and more atoms are populated in the $3p^5 4s$ excited state as compared to the $3p^5 4p$ excited state. In Fig. 4(b), we can clearly see that the ionization energies of these excited states are much lower than that of the ground state, and thus the nonlinear susceptibility can be significantly promoted through the gas excitation.

To confirm the crucial role of the excited states on the harmonic enhancement, we further measured the absorption dynamics. The absorption coefficient, defined as $\alpha = -\ln(I_{\text{out}}/I_{\text{in}})$, is approximately proportional to the population in the lower state when the population in the upper state is negligible. In this case, we can obtain the population dynamics of the excited $3p^5 4s$ state by scanning the delay of the weak 800-nm probe pulse and the 1420-nm prepulse. As demonstrated in Fig. 3(b), the phase mismatch can be ignored in this experiment. Thus, the 7th-harmonic yield has a squared dependence on the population of the excited state as well as the absorption coefficient α. For a direct comparison with the enhancement dynamics in Fig. 2(b), we depict the evolution of α^2 with the time delay in Fig. 5. It can be seen that the measured α^2 for each transition follows a similar temporal evolution with the enhanced harmonic radiation. The good agreement between Figs. 2(b) and 5 indicates that the 7th-harmonic enhancement in two stages is mainly attributed to the generation of the $3p^5 4s$ excited state.

D. Pathways responsible for the excited-state generation

In this section, we will explore the possible pathways responsible for generation of the $3p^5 4s$ state. First, the photoexcitation from the ground $3p^6$ state to the excited $3p^5 4s$ state can be excluded. This is because the excited state generated by multiphoton excitation would be populated to maximum after the laser field, which apparently is not our case. In addition, Rydberg-state atoms produced through frustrated tunneling ionization or electron recollisional excitation would have extremely low population since we adopt the circularly polarized pre-excited pulses in this experiment [40]. Thus, we can also exclude the possibility of population relaxation from high Rydberg states to the first excited state $3p^5 4s$.

One possible pathway to generate the excited state is electron impact excitation, which is realized by the collision of a hot electron with its surrounding atoms. This process can be expressed as

$$e + \text{Ar} \rightarrow e + \text{Ar}^*(3p^5 4s). \tag{1}$$

For this process, the collision rate coefficient is calculated by $k = 1.45 \times 10^{-8} e^{-12.96/T_e}\ \text{cm}^3/\text{s}$ [41,42]. The average kinetic energy of the electron T_e obtained from a circularly polarized laser field is estimated to be 18.8 eV with the laser intensity of $5 \times 10^{13}\ \text{W/cm}^2$ [34]. The corresponding rate coefficient is $\sim 7 \times 10^{-9}\ \text{cm}^3/\text{s}$. The number density of argon atoms ρ is taken as $\sim 1 \times 10^{19}\ \text{cm}^{-3}$ at the gas pressure of 400 mbar. Thus, the collision rate is determined to be $\Gamma = \rho k = 7 \times 10^{10}\ \text{s}^{-1}$. The collision time between hot electrons and Ar atoms is about 14 ps. The excited atoms are easily ionized through the electron impact, which would give rise to the fast decay of population in the excited state [33,41]. In addition, the electron energy will significantly decrease after several picoseconds [43], which will strongly influence the efficiency of electron impact excitation. Therefore, the generation and dissipation processes of the excited state as well as the rapid decay of the electron energy could result in the maximum population of the excited state at several picoseconds after the prepulse, as shown in Figs. 5(a)–5(c).

It is noteworthy that the electron impact excitation from ground state to other higher excited states, especially the $3p^5 4p$ state, is also very efficient. In this perspective, the absorption dynamics on the picosecond timescale could reflect the population difference between $3p^5 4s$ and $3p^5 4p$ states, which could result in the difference between the harmonic enhancement dynamics in Fig. 2(b) and the absorption dynamics in Fig. 5. In addition, the temporal evolutions of three absorption lines also have small differences, as shown in Figs. 5(a)–5(c). This could be because the cross sections of electron impact excitation are different for each sublevel of the $3p^5 4s$ and $3p^5 4p$ states [44]. Therefore, the quantitative calculation of the population dynamics requires one to solve the rate equation with the cross sections of these specific energy levels and consider all possible pathways on the picosecond timescale, which is beyond the scope of this work.

At the time delay of several nanoseconds, both the electron energy and electron density are significantly reduced, and thus the pathway of electron collisional excitation will close. In this case, the excited state can be created by the three-body collisions and the subsequent dissociative recombination, which are described as

$$\text{Ar}^+ + 2\text{Ar} \rightarrow \text{Ar}_2{}^+ + \text{Ar}, \tag{2}$$

$$\text{Ar}_2{}^+ + e \rightarrow \text{Ar}^*(3p^5 4s) + \text{Ar}. \tag{3}$$

This pathway has been investigated in the nitrogen laser in the N_2/Ar gas mixture, where the population inversion of nitrogen molecules is created by the collision of argon atoms at the $3p^5 4s$ excited state and nitrogen molecules [45]. By solving rate equations, it is theoretically demonstrated that the population of the $3p^5 4s$ state reaches the maximum on the nanosecond timescale [45], which is comparable to the timescale of the population inversion. The experimental measurement on gain dynamics of nitrogen lasers agrees well with the simulation results [46]. Therefore, the generation of the $3p^5 4s$ excited state on the nanosecond timescale probably originates from the above two-step processes, i.e., the three-body collisions and the subsequent dissociative recombination.

IV. CONCLUSION AND OUTLOOK

In conclusion, we have observed the dramatic enhancement of 7th-harmonic generation in the argon gas by injecting an intense prepulse ahead of the driver pulse. By measuring the evolution of enhanced harmonic radiations along the propagation medium, we distinguished the contributions of improved phase matching and enhanced nonlinear susceptibility to the harmonic enhancement. The time- and spectrum-resolved measurements of the excited medium clearly demonstrated that generation of the excited argon atoms results in a higher nonlinear susceptibility, which makes a crucial contribution to the harmonic enhancement. This work clarifies the physical origin of the enhanced optical nonlinearity, and reveals the complex dynamics of laser-induced plasma, which is of great importance for optimizing the generation of coherent ultrafast pulses at short wavelengths. Furthermore, this all-optical method is simple, and there is no special requirement for laser wavelengths. In principle, it can be applied to a wide range of atoms or molecules, as well as high-order harmonic generation at extreme ultraviolet and even x-ray wavelengths.

ACKNOWLEDGMENTS

This work is supported by National Key Research and Development Program of China (Grant No. 2018YFB0504400); National Natural Science Foundation of China (Grants No. 11822410, No. 11734009, and No. 61575211); Strategic Priority Research Program of Chinese Academy of Sciences (Grant No. XDB16030300); Key Research Program of Frontier Sciences, Chinese Academy of Sciences (Grant No. QYZDJ-SSW-SLH010); Key Project of the Shanghai Science and Technology Committee (Grant No. 18DZ1112700); Shanghai Rising-Star Program (Grant No. 17QA1404600); and Youth Innovation Promotion Association of Chinese Academy of Sciences (Grant No. 2018284).

[1] S. Backus, J. Peatross, Z. Zeek, A. Rundquist, G. Taft, M. M. Murnane, and H. C. Kapteyn, Opt. Lett. **21**, 665 (1996).
[2] N. Aközbek, A. Iwasaki, A. Becker, M. Scalora, S. L. Chin, and C. M. Bowden, Phys. Rev. Lett. **89**, 143901 (2002).
[3] F. Théberge, N. Aközbek, W. Liu, J.-F. Gravel, and S. L. Chin, Opt. Commun. **245**, 399 (2005).
[4] F. Théberge, N. Aközbek, W. Liu, A. Becker, and S. L. Chin, Phys. Rev. Lett. **97**, 023904 (2006).
[5] H. Xiong, H. Xu, Y. Fu, Y. Cheng, Z. Xu, and S. L. Chin, Phys. Rev. A **77**, 043802 (2008).
[6] T. Popmintchev, M.-C. Chen, D. Popmintchev, P. Arpin, S. Brown, S. Ališauskas, G. Andriukaitis, T. Balciunas, O. D. Mücke, A. Pugzlys, A. Baltuška, B. Shim, S. E. Schrauth, A. Gaeta, C. Hernández-García, L. Plaja, A. Becker, A. Jaron-Becker, M. M. Murnane, and H. C. Kapteyn, Science **336**, 1287 (2012).
[7] G. Li, J. Ni, H. Xie, B. Zeng, J. Yao, W. Chu, H. Zhang, C. Jing, F. He, H. Xu, Y. Cheng, and Z. Xu, Opt. Lett. **39**, 961 (2014).
[8] R. Ackermann, E. Salmon, N. Lascoux, J. Kasparian, P. Rohwetter, K. Stelmaszczyk, S. Li, A. Lindinger, L. Wötse, P. Béjot, L. Bonacina, and J. P. Wolf, Appl. Phys. Lett. **89**, 171117 (2006).
[9] C.-C. Kuo, C.-H. Pai, M.-W. Lin, K.-H. Lee, J.-Y. Lin, J. Wang, and S.-Y. Chen, Phys. Rev. Lett. **98**, 033901 (2007).
[10] B. Shim, G. Hays, R. Zgadzaj, T. Ditmire, and M. C. Downer, Phys. Rev. Lett. **98**, 123902 (2007).
[11] E. Schulz, D. S. Steingrube, T. Vockerodt, T. Binhammer, U. Morgner, and M. Kovačev, Opt. Lett. **36**, 4389 (2011).
[12] T. T. Xi, X. Lu, and J. Zhang, Opt. Commun. **282**, 3140 (2009).
[13] Z. Zhang, X. Lu, Y. Zhang, M. Zhou, T. Xi, Z. Wang, and J. Zhang, Opt. Lett. **35**, 974 (2010).
[14] K. Hartinger and R. A. Bartels, Appl. Phys. Lett. **93**, 151102 (2008).
[15] S. Suntsov, D. Abdollahpour, D. G. Papazoglou, and S. Tzortzakis, Opt. Express **17**, 3190 (2009).
[16] X. Yang, J. Wu, Y. Peng, Y. Tong, S. Yuan, L. Ding, Z. Xu, and H. Zeng, Appl. Phys. Lett. **95**, 111103 (2009).
[17] Y. Liu, M. Durand, A. Houard, B. Forestier, A. Couairon, and A. Mysyrowicz, Opt. Commun. **284**, 4706 (2011).
[18] Z. Liu, P. Ding, Y. Shi, X. Lu, S. Sun, X. Liu, Q. Liu, B. Ding, and B. Hu, Opt. Express **20**, 8837 (2012).
[19] J. Yao, B. Zeng, W. Chu, J. Ni, and Y. Cheng, J. Mod. Opt. **59**, 245 (2012).
[20] Z. Liu, P. Ding, Y. Shi, X. Lu, Q. Liu, S. Sun, X. Liu, B. Ding, and B. Hu, Laser Phys. Lett. **9**, 649 (2012).
[21] L. Shi, W. Li, H. Zhou, D. Wang, L. Ding, and H. Zeng, Appl. Phys. Lett. **102**, 081112 (2013).
[22] V. Vaičaitis, V. Jarutis, K. Steponkevičius, and A. Stabinis, Phys. Rev. A **87**, 063825 (2013).
[23] P. J. Ding, Z. Y. Liu, Y. C. Shi, S. H. Sun, X. L. Liu, X. Sh. Wang, Z. Q. Guo, Q. C. Liu, Y. H. Li, and B. T. Hu, Phys. Rev. A **87**, 043828 (2013).
[24] D. Wang, W. Li, L. Ding, and H. Zeng, Opt. Lett. **39**, 4140 (2014).
[25] H. Xie, G. Li, J. Yao, W. Chu, Z. Li, B. Zeng, Z. Wang, and Y. Cheng, Sci. Rep. **5**, 16006 (2015).
[26] A. Nath, J. A. Dharmadhikari, D. Mathur, and A. K. Dharmadhikari, Appl. Phys. B **122**, 248 (2016).
[27] G. Li, H. Xie, Z. Li, J. Yao, W. Chu, and Y. Cheng, High Power Laser Sci. Eng. **5**, e26 (2017).
[28] P. Wei, X. Yuan, C. Liu, Z. Zeng, Y. Zheng, J. Jiang, X. Ge, and R. Li, Opt. Express **23**, 17229 (2015).

[29] X. Yuan, P. Wei, C. Liu, Z. Zeng, Y. Zheng, J. Jiang, X. Ge, and R. Li, Appl. Phys. Lett. **107**, 041110 (2015).
[30] S. Suntsov, D. Abdollahpour, D. G. Papazoglou, and S. Tzortzakis, Phys. Rev. A **81**, 033817 (2010).
[31] C. Rodríguez, Z. Sun, Z. Wang, and W. Rudolph, Opt. Express **19**, 16115 (2011).
[32] L. Feng, X. Lu, T. Xi, X. Liu, Y. Li, L. Chen, J. Ma, Q. Dong, W. Wang, Z. Sheng, D. He, and J. Zhang, Phys. Plasmas **19**, 072305 (2012).
[33] P. Wei, M. Qin, K. E. Dorfman, X. Yuan, C. Liu, Z. Zeng, X. Ge, X. Zhu, Q. Liang, B. Yao, Q. J. Wang, H. Li, J. Liu, Y. Zhang, S. Y. Jeong, G. S. Yun, D. E. Kim, P. Lu, and R. Li, Opt. Lett. **43**, 1970 (2018).
[34] K. E. Dorfman, P. Wei, J. Liu, and R. Li, Opt. Express **27**, 7147 (2019).
[35] N. A. Papadogiannis, C. Kalpouzos, E. Goulielmakis, G. Nersisyan, D. Charalambidis, F. Augé, F. Weihe, and Ph. Balcou, Appl. Phys. B **73**, 687 (2001).
[36] J. Peatross, J. R. Miller, K. R. Smith, S. E. Rhynard, and B. W. Pratt, J. Mod. Opt. **51**, 2675 (2004).
[37] J.-P. Brichta, M. C. H. Wong, J. B. Bertrand, H.-C. Bandulet, D. M. Rayner, and V. R. Bhardwaj, Phys. Rev. A **79**, 033404 (2009).
[38] R. W. Boyd, *Nonlinear Optics* (Elsevier, Amsterdam, 2008).
[39] J. B. Boffard, R. O. Jung, C. C. Lin, and A. E. Wendt, Plasma Sources Sci. Technol. **18**, 035017 (2009).
[40] L. Zhao, J. Dong, H. Lv, T. Yang, Y. Lian, M. Jin, H. Xu, D. Ding, S. Hu, and J. Chen, Phys. Rev. A **94**, 053403 (2016).
[41] X. Gao, G. Patwardhan, S. Schrauth, D. Zhu, T. Popmintchev, H. C. Kapteyn, M. M. Murnane, D. A. Romanov, R. J. Levis, and A. L. Gaeta, Phys. Rev. A **95**, 013412 (2017).
[42] E. Eggarter, J. Chem. Phys. **62**, 833 (1975).
[43] P. Ding, E. Oliva, A. Houard, A. Mysyrowicz, and Y. Liu, Phys. Rev. A **94**, 043824 (2016).
[44] A. Yanguas-Gil, J. Cotrino, and L. L. Alves, J. Phys. D: Appl. Phys. **38**, 1588 (2005).
[45] M. N. Shneider, A. Bakuška, and A. M. Zheltikov, J. Appl. Phys. **110**, 083112 (2011).
[46] H. Xie, G. Li, W. Chu, B. Zeng, J. Yao, C. Jing, Z. Li, and Y. Cheng, New J. Phys. **17**, 073009 (2015).